A magnetized object in Kaluza–Klein theory

K. D. Krori and J. C. Sarmah
Mathematical Physics Forum, Cotton College, Gauhati 781001, India
Received August 22, 1989

In this paper, we present a study of the stable equatorial ($\theta = \pi/2$) and polar (ϕ = constant) trajectories of neutral or charged test particles around a magnetized object in five-dimensional Kaluza–Klein theory. We also show how the nature of these trajectories changes with the variation of the angular momentum of the test particles and with the magnetic-field parameter. We point out that the Gaussian curvature tends to infinity at the Matos surface (defined in the text). A comparison is also made between four-dimensional and five-dimensional studies for equatorial and polar trajectories.

Dans cet article, nous présentons une étude des trajectoires stables équatoriales ($\theta = \pi/2$) et polaires (ϕ = const.) de particules d'essai, neutres ou chargées, autour d'un objet aimanté, dans la théorie Kaluza–Klein à cinq dimensions. Nous montrons aussi que la nature de ces trajectoires change avec la variation du moment cinétique des particules d'essai et du paramètre de champ magnétique. Nous montrons que la courbure gaussienne tend vers l'infini à la surface de Matos (définie dans le texte). On fait aussi une comparaison entre les théories à quatre et à cinq dimensions pour les trajectoires équatoriales et polaries.

[Traduit par la revue]

Can. J. Phys. 68, 649 (1990)

1. Introduction

During the past two decades, a lot of attention has been devoted to the study of particle trajectories in the fields of astrophysical objects embedded in magnetic or gravitational fields. Dadhich *et al.* (1) studied the trajectories of charged particles in the equatorial plane of the Ernst space-time (2). Dhurandhar and Sharma (3) considered null geodesics in the same space-time. Krori and Sarmah (4) investigated the stability of trajectories of superluminal particles (tachyons) in the equatorial plane of the Ernst space-time. Later Krori *et al.* (5) showed that stable trajectories of charged particles, neutral particles, photons, and tachyons occur in the equatorial plane of the Ernst space-time. More recently, Krori and Sarmah have worked on studies of the distorted polar trajectories of neutral particles around a black hole embedded in (*i*) a magnetic (6) and (*ii*) a gravitational field (7).

But so far, no investigation has been made, to our knowledge, of the field of an astrophysical object in five-dimensional Kaluza–Klein theory. The purpose of this paper is to present a study, using neutral or changed test particles, of the equatorial and the polar fields of a magnetized object in this theory. We also show how the nature of these trajectories changes with the angular momentum of the test particle and the magnetic-field parameter and we point out that the Gaussian curvature tends to infinity at the Matos surface (defined in Sect. 5). In Sect. 6, a study in five dimensions is added for a comparison with the results in four dimensions.

2. Effective potential and stability

The four-dimensional metric representing a magnetized object in five-dimensional Kaluza–Klein theory is given by Matos (8) as follows

$$[1]\qquad ds^2 = \left(1-\frac{2m}{r}\right)^{1/2}\left[1-\log_e\left(1-\frac{2m}{r}\right)^{1/2}\right]\left\{\left[1-\frac{m^2\sin^2\theta}{r^2\left(1-\frac{2m}{r}\right)}\right]^{1/4}\left[\frac{dr^2}{\left(1-\frac{2m}{r}\right)}+r^2\,d\theta^2\right]+r^2\sin^2\theta\,d\phi^2\right\}-\left(1-\frac{2m}{r}\right)dt^2$$

For convenience we may write $[1-(2m/r)] = \chi$. Then [1] may be written as

$$[2]\qquad ds^2 = \chi^{1/2}[1-\eta\log_e\chi^{1/2}]\left\{\left[1-\frac{m^2\sin^2\theta}{r^2\chi}\right]^{1/4}\left(\frac{dr^2}{\chi}+r^2\,d\theta^2\right)+r^2\sin^2\theta\,d\phi^2\right\}-\chi\,dt^2$$

where η is the magnetic-field parameter related to the magnetic potential, A_ϕ, given by

$$[3]\qquad A_\phi = -\eta m\cos\theta$$

From [2] we have

$$g^{00} = \frac{1}{\chi}$$

[4]
$$g^{11} = \chi^{1/2}(1 - \eta \log_e \chi^{1/2})^{-1}\left(1 - \frac{m^2 \sin^2\theta}{r^2\chi}\right)^{-1/4}$$

$$g^{22} = r^{-2}\chi^{-1/2}(1 - \eta \log_e \chi^{1/2})^{-1}\left(1 - \frac{m^2 \sin^2\theta}{r^2\chi}\right)^{-1/4}$$

$$g^{33} = \chi^{-1/2}r^{-2}\sin^{-2}\theta(1 - \eta \log_e \chi^{1/2})^{-1}$$

For a particle of mass μ and charge e we have (9)

[5a]
$$-\mu^2 = g^{\alpha\beta}p_\alpha p_\beta$$
$$= g^{11}p_r^2 + g^{22}p_\theta^2 + g^{33}p_\phi^2 + g^{00}p_0^2$$

where

p_r = the r component of four-momentum

p_θ = the θ component of four- momentum

[5b] p_ϕ = the ϕ component of four-momentum

$$= r^2\chi^{1/2}(1 - \eta \log_e \chi^{1/2})\sin^2\theta\dot{\phi}$$
$$= L_e - eA_\phi$$

L_e is the angular momentum about the axis of symmetry, e is the charge of a test particle in the field of the object, and p_0 is the t component of the four-momentum, that is, ε (say).

In the equatorial plane $\theta = \pi/2$, $p_\theta = 0$ [5a] gives

[6]
$$\varepsilon^2 \equiv E = \frac{g^{11}}{g^{00}}\left(\frac{\partial r}{\partial\phi}\right)^2\dot{\phi}^2 + \frac{1}{g^{00}}[g^{33}L_e^2 + \mu^2]$$
$$= \frac{g^{11}}{g^{00}}\left(\frac{\partial r}{\partial\phi}\right)^2\dot{\phi}^2 + \chi\left[\frac{L_e^2}{r^2\chi^{1/2}(1 - \eta \log_e \chi^{1/2})} + \mu^2\right]$$

where a dot means differentiation with respect to an affine parameter λ. Then,

$$E = \frac{g^{11}}{g^{00}}\left(\frac{\partial r}{\partial\phi}\right)^2\dot{\phi}^2 + V_e(r)$$

where the effective potential function is

[7]
$$V_e(r) = \frac{L_e^2\chi^{1/2}}{r^2(1 - \eta \log_e \chi^{1/2})} + \chi\mu^2$$

Using [7] we have calculated the effective potential function $V_e(r)$ vs. r for various values of L_e with $m = 1$, $\mu^2 = 1$, and $\eta = 0.09$ for the test particles. These results are plotted in Fig. 1. These curves show distinct positive minima, which indicate the stability of orbits. Then results for $V_e(r)$ vs. r are calculated for the particles with $m = 1$, $\mu^2 = 1$, and $L_e = 10$ for various values of η. These results are plotted in Fig. 2. The calculations and the plots show distinct positive minima, which indicate the stability of orbits in the equatorial ($\theta = \pi/2$) plane.

3. Bound equatorial orbit

The nature of the bound orbit in the equatorial ($\theta = \pi/2$) plane is obtained by considering [6]. Using the values of g^{00}, g_{11}, and $\dot{\phi}$ from [4], [2], and [5b] in [6] we obtain

$$\left(\frac{\partial r}{\partial\phi}\right)^2 = \frac{[E - V_e(r)]r^4\chi^{1/2}(1 - \eta \log_e \chi^{1/2})}{L_e^2\left(1 - \frac{m^2}{r^2\chi}\right)^{1/4}}$$

Hence

[8]
$$\frac{\partial r}{\partial\phi} = \frac{[E - V_e(r)]^{1/2}r^2\chi^{1/4}(1 - \eta \log_e \chi^{1/2})^{1/2}}{L_e\left(1 - \frac{m^2}{r^2\chi}\right)^{1/8}}$$

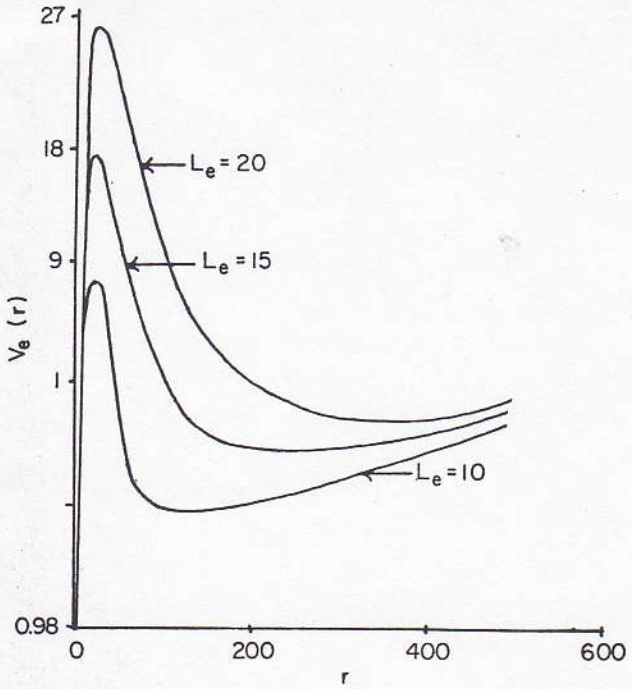

FIG. 1. Plot of $V_e(r)$ vs. r for various values of L_e with $m = 1$, $\mu^2 = 1$, and $\eta = 0.09$.

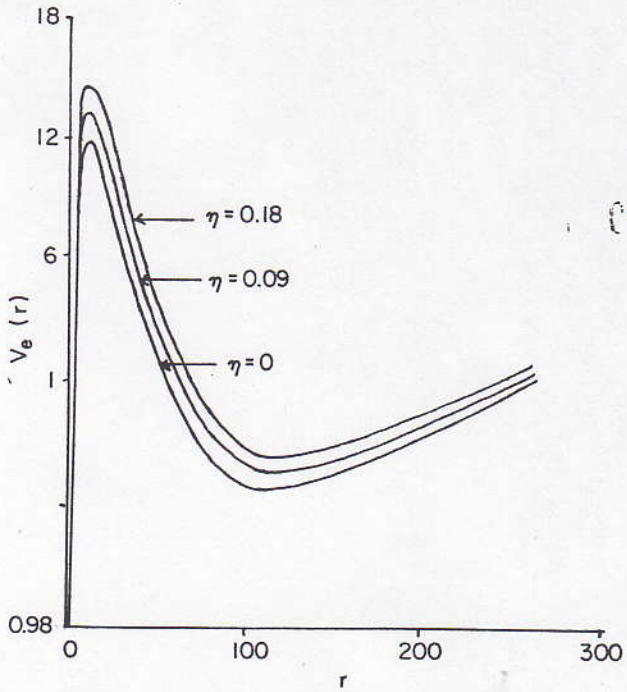

FIG. 2. Plot of $V_e(r)$ vs. r for various values of η with $m = 1$, $\mu^2 = 1$, and $L_e = 10$.

Using [8] and putting $\eta = 0.09$, $m = 1$, $L_e = 10$, and $E = 0.9955$ we calculate the orbit. The nature of the orbit is spiral and confined between the radii $r = r_1$ and $r = r_2$ as shown in Fig. 3.

4. Polar orbit

To find the nature of a polar orbit (ϕ = constant plane), we use [5]. Considering $p_\phi = 0$ and $p_\theta = L_p$, the angular momentum of the test particle in a polar orbit, we find the expression for the effective potential in the ϕ =constant plane is

$$[9] \qquad V_p(r,\theta) = \frac{L_p^2 \chi^{1/2}}{r^2\left(1 - \frac{m^2 \sin^2\theta}{r^2\chi}\right)^{1/4}(1 - \eta \log_e \chi^{1/2})} + \chi\mu^2$$

Considering $m = 1$, $\mu^2 = 1$, and $L_p = 10$ we calculate the values of the potential functions using [9] for different values of η ($\eta = 0.00$, 0.09, and 0.18) with various values of θ ($\theta = 0$–2π). The minima are shown in Table 1. The values of the minima (r_m) thus obtained are joined for each value of η and elliptical curves are obtained. The nature of the curves are represented in Fig. 4.

Next using $m = 1$, $\mu^2 = 1$, and $\eta = 0.09$ we calculate the values of V_p (r, θ) for various values of L_p (L_p = 10, 15, and 20) for $\theta = 0$–2π. The values of r_m that correspond to the minima thus obtained are shown in Table 2. Joining these values of r_m for each value of L_p we get elliptical curves, the nature of which are represented in Fig. 5.

5. Gaussian curvature at the Matos surface

The metric [1] shows that for

$$[10] \qquad r_m = m + m\sqrt{1 + \sin^2\theta}$$

the expression

$$[11] \qquad 1 - \frac{m^2 \sin^2\theta}{r^2\left(1 - \frac{2m}{r}\right)} = 0$$

The expression in [11] becomes imaginary for

$$r < r_M$$

We call the surface corresponding to $r = r_M$ (see [10]) the Matos surface after the author of metric [1]. We now proceed to find the Gaussian curvature at this surface using the two-dimensional line element

$$[12] \qquad ds_I^2 = H\, d\theta^2 + G\, d\phi^2$$

TABLE 1. Values of r_m for various values of η with $m = 1$, $L_p = 10$ and $\mu^2 = 1$

η	0° 360°	30° 330°	45° 315°	60° 300°	90° 270°	120° 240°	135° 225°	150° 210°	180° 0°
0.00	222.4	222.6	222.7	222.8	223	222.8	222.7	222.6	222.4
0.09	223	223.3	223.5	223.7	224.1	223.7	223.5	223.3	223
0.18	224	224.25	224.5	224.8	225.2	224.8	224.5	224.25	224

TABLE 2. Values of r_m for various values of L_p with $\eta = 0.09$, $m = 1$, and $\mu^2 = 1$

L_p	0° 360°	30° 330°	45° 315°	60° 300°	90° 270°	120° 240°	135° 225°	150° 210°	180° 0°
10	98.8	98.81	98.85	98.87	98.9	98.87	98.85	98.81	98.8
15	223	223.3	223.5	223.7	224.1	223.7	223.5	223.3	223
20	398	398.4	399	399.6	400	399.6	399	398.4	398

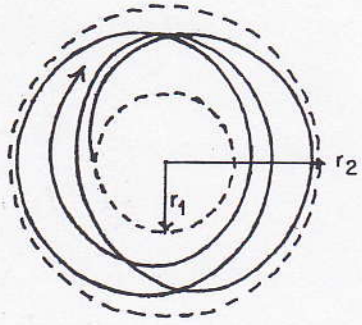

FIG. 3. Nature of equatorial orbits of the test particles.

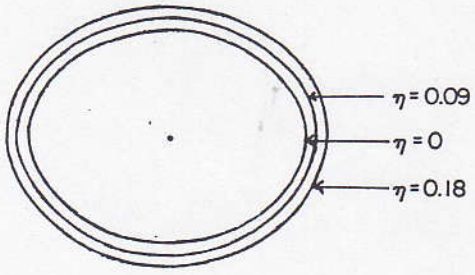

FIG. 4. Nature of polar orbits of the test particles with $m = 1$, $\mu^2 = 1$, and $L_p = 10$ for various values of η.

where

$$[13] \quad H = r^2\chi^{1/2}(1 - \eta \log_e \chi^{1/2})\left(1 - \frac{m^2 \sin^2\theta}{r^2\chi}\right)^{1/4}$$

and

$$[14] \quad G = r^2\chi^{1/2}(1 - \eta \log_e \chi^{1/2})\sin^2\theta$$

The Gaussian curvature at any given value of r is given by

$$[15] \quad K = -\frac{1}{2\sqrt{HG}} \frac{d}{d\theta}\left[\frac{1}{\sqrt{HG}} \frac{dG}{d\theta}\right]$$

Substituting [13] and [14] in [15] we obtain

$$[16] \quad K = \frac{4r^2\chi\left(1 - \frac{m^2 \sin^2\theta}{r^2\chi}\right) - m^2 \cos\theta}{4r^4\chi^{3/2}(1 - \eta \log_e \chi^{1/2})\left(1 - \frac{m^2 \sin^2\theta}{r^2\chi}\right)^{5/4}}$$

It can be seen that as r tends to r_M, K tends to infinity. This is an important feature of the Matos surface. Another peculiar feature of this surface is that it exhibits singularity only at two points $r_M = 2m$, $\theta = 0$ and $r_M = 2m$, $\theta = \pi$.

6. A study in five dimensions

Following Gegenberg and Kunstatter (10), the Matos metric [1] may be written in five dimensions

$$[17] \quad ds^2 = g_{\mu\nu}\, dx^\mu\, dx^\nu + l^2(A_\mu\, dx^\mu + dx^5)^2$$

where $\mu, \nu = 0, 1, 2, 3,$

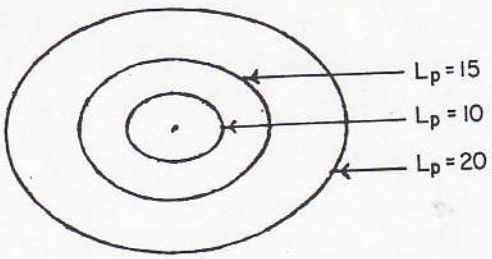

FIG. 5. Nature of polar orbits of the test particles with $m = 1$, $\mu^2 = 1$, and $\eta = 0.09$ for various values of L_p.

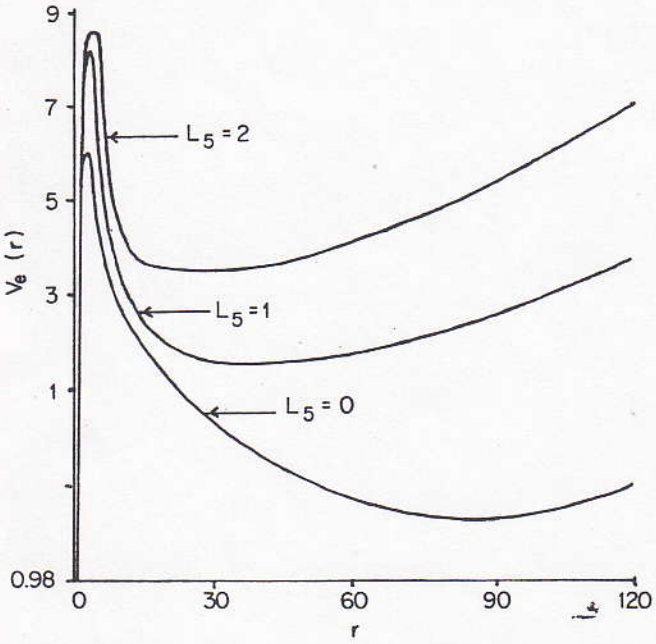

FIG. 6. Plot of $V_e(r)$ for various values of L_5 with $\mu^2 = 1$, $m = 1$, $L_e = 10$, and $\eta = 0.09$.

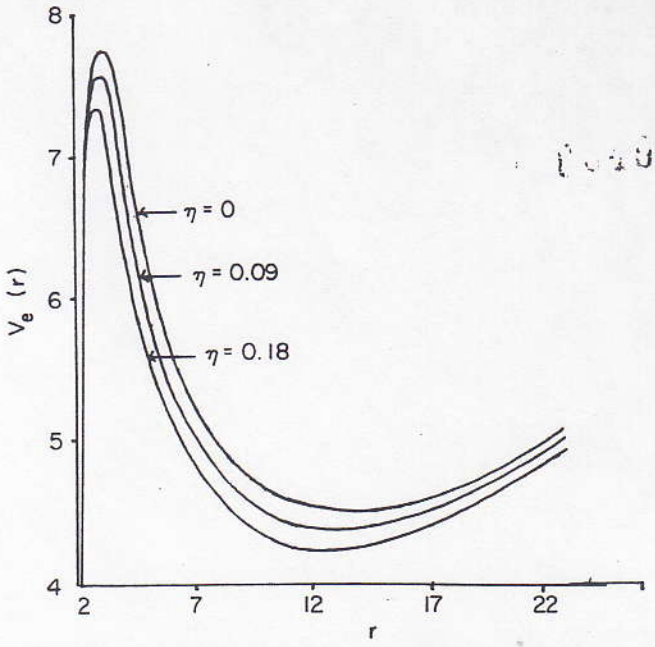

FIG. 7. Plot of $V_e(r)$ for various values of η with $\mu^2 = 1$, $m = 1$, $L_e = 10$, and $L_5 = 2$.

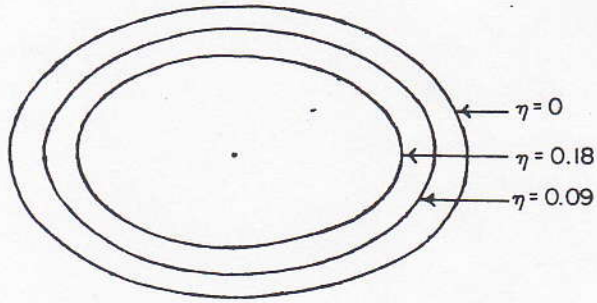

FIG. 8. Polar orbits for various values of η with $\mu^2 = 1$, $m = 1$, $L_p = 10$, and $L_5 = 2$.

[18] $$I^2(\text{scalar field}) = \frac{1}{\left(1-\frac{2m}{r}\right)^{1/2}\left[1-\eta\log_e\left(1-\frac{2m}{r}\right)^{1/2}\right]}$$

and $A_0 = A_1 = A_2 = 0$, $A_3 = -\eta m\cos\theta$

Also following ref 10, we have

[19] $$-\mu^2 = g^{00}p_0^2 + g^{11}P_r^2 + g^{33}p_\phi^2 + \frac{L_5^2}{I^2}$$

for equatorial trajectories with L_5 equal to the angular momentum in the fifth dimension and

[20] $$-\mu^2 = g^{00}p_0^2 + g^{11}p_r^2 + g^{22}p_\theta^2 + \frac{L_5^2}{I^2}$$

for polar trajectories. Corresponding to [19] the potential-energy function for an equatorial trajectory is (see [7])

[21] $$V_e(r) = \frac{L_e^2\chi^{1/2}}{r^2(1-\eta\log_e\chi^{1/2})} + \chi\left(\mu^2 + \frac{L_5^2}{I^2}\right)$$

On the other hand, corresponding to [20], the potential-energy function for a polar trajectory is (see [9])

[22] $$V_p(r,\theta) = \frac{L_p^2\chi^{1/2}}{r^2\left(1-\frac{m^2\sin^2\theta}{r^2\chi}\right)^{1/4}(1-\eta\log_e\chi^{1/2})} + \chi\left(\mu^2 + \frac{L_5^2}{I^2}\right)$$

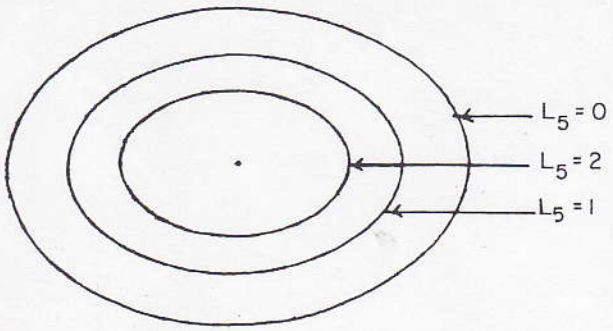

FIG. 9. Polar orbits for various values of L_5 with $\mu^2 = 1$, $m = 1$, $L_p = 10$, and $\eta = 0.09$.

As pointed out in ref 10, L_5 is related to the charge of the test particle. Equations [21] and [22], therefore, show that the potential-energy function are the same in both four and five dimensions for uncharged particles. Differences occur, however, for charged test particles as shown in Figs. 6–9.

7. Discussion

The analysis in four dimensions leads us to the conclusion that massive test particles may move around a Kaluza–Klein object in stable equatorial and polar (ϕ = constant) orbits. A special feature of polar orbits is that they are a little flattened at the poles whereas the stable polar orbits in refs. 6 and 7 are elongated at the poles. Another interesting feature of our investigation is that the equatorial and polar orbits are the same for both charged and neutral particles. Also it is clear from Sect. 5 that the metric [1] is not valid for $r < r_M$ (see [10]) and the Gaussian curvature tends to infinity for r tending to r_M.

However, the results are different for charged ($L_5 \neq 0$) particles in five dimensions. Figure 6 shows how the nature of $V_e(r)$ changes for different values of L_5 ($L_5 = 0, 1$, and 2) with $\mu^2 = 1$, $m = 1$, $L_e = 10$, and $\eta = 0.09$. On the other hand, with $\mu^2 = 1$, $m = 1$, and $L_e = 10$ the order of the curves in Fig. 2 for $L_5 = 0$ in four dimensions is exactly reversed in Fig. 7 for $L_5 = 2$ in five dimensions. Also, a reversal of the order of the curves in Fig. 4 for $L_5 = 0$ in four dimensions occurs in Fig. 8 for $L_5 = 2$ in five dimensions. Figure 9 shows that the orbit with $\mu^2 = 1$, $m = 1$, $L_p = 10$, and $\eta = 0.09$ becomes smaller and smaller as L_5 increases from $0 \longrightarrow 1 \longrightarrow 2$.

Acknowledgements

The authors express their profound gratitude to the Government of Assam for providing all facilities at Cotton College, Gauhati 781001, India. These facilities have enabled us to carry out the investigations reported in this paper.

1. N. DADHICH, C. HOENSELAERS, and C. V. VISHVESHWARA. J. Phys. A: Math. Gen. **12**, 215 (1979).
2. F. J. ERNST. J. Math. Phys. (N.Y.), **17**, 54 (1976).
3. S. V. DHURANDHAR and D. N. SARMA. J. Phys. A: Math. Gen. **16**, 99 (1983).
4. K. D. KRORI and J. C. SARMAH. Can. J. Phys. **63**, 646 (1985).
5. K. D. KRORI, R. CHOUDHURY, and J. C. SARMAH. Can. J. Phys. **64**, 1455 (1986).
6. K. D. KRORI and J. C. SARMAH. Can. J. Phys. **67**, 971 (1989).
7. K. D. KRORI and J. C. SARMAH. Can. J. Phys. **67**, 505 (1989).
8. T. MATOS. Phys. Rev. D: Part. Fields, **38**, 3008 (1988).
9. C. W. MISNER, K. S. THORNE, and J. A. WHEELER. Gravitation. W. H. Freeman and Co., San Francisco. 1973. p. 649.
10. J. GEGENBERG and G. KUNSTATTER. Phys. Lett. **106A**, 410 (1984).